

## Article

# Biogenic Silver and Copper Nanoparticles: Potential Antifungal Agents in Rice and Wheat Crops

Paula Sanguineto <sup>1</sup>, Ricardo Faccio <sup>2</sup> , Eduardo Abreo <sup>3</sup> and Silvana Alborés <sup>1,\*</sup> 

<sup>1</sup> Área de Microbiología, Departamento de Biociencias, Facultad de Química, Universidad de la República, Montevideo 11800, Uruguay; paulasd.92@gmail.com

<sup>2</sup> Centro NanoMat & Grupo Física, Departamento de Experimentación y Teoría de la Estructura de la Materia y sus Aplicaciones (DETEMA), Facultad de Química, Universidad de la República, Montevideo 11800, Uruguay; rfaccio@fq.edu.uy

<sup>3</sup> Plataforma de Bioinsumos, Estación Experimental INIA Las Brujas, Instituto Nacional de Investigación Agropecuaria, Canelones 90100, Uruguay; eabreo@inia.org.uy

\* Correspondence: salbores@fq.edu.uy; Tel.: +598-29244209

**Abstract:** Metal nanoparticles are widely studied due to their various applications, such as their potential use in the control of phytopathogens and the promotion of plant growth, with a significant impact on agriculture. Various microbial metabolites are used to reduce and stabilize metals and metal oxides to the nanoscale. In the present work, the biological synthesis of silver and copper oxide nanoparticles using *Trichoderma harzianum* TA2 is reported. The nanoparticles were purified and characterized with complementary methodologies to obtain information on the size, distribution, morphology, surface charge, and functional groups of the nanoparticles. The in vitro antifungal activity of the nanoparticles against pathogens of rice and wheat, as well as their effect on seed germination, were evaluated. In general, the nanoparticles showed a spherical shape, an average size of 17–26 nm, and low polydispersity. Furthermore, they showed antifungal activity at low concentrations against *Sclerotium oryzae* (0.140  $\eta$ M), *Rhizoctonia oryzae-sativae* (0.140  $\eta$ M), *Fusarium graminearum* (0.034  $\eta$ M), and *Pyricularia oryzae* (0.034  $\eta$ M). The germination of seeds treated with nanoparticles was not negatively affected. This is the first report of biogenic silver and copper oxide nanoparticles from a single strain of *T.harzianum* with antifungal activity against four phytopathogens of interest in Uruguay. Furthermore, the synthesis of the biogenic nanoparticles was faster and more efficient than previous reports using other fungi. In conclusion, this work reveals that biogenic metallic nanoparticles from *T. harzianum* TA2 can be considered as candidates for the control of phytopathogens affecting important crops.

**Keywords:** biogenic nanoparticles; *Trichoderma*; antifungal; phytopathogens



**Citation:** Sanguineto, P.; Faccio, R.; Abreo, E.; Alborés, S. Biogenic Silver and Copper Nanoparticles: Potential Antifungal Agents in Rice and Wheat Crops. *Chemistry* **2023**, *5*, 2104–2119. <https://doi.org/10.3390/chemistry5040143>

Academic Editor: Simona Concilio

Received: 5 August 2023

Revised: 2 October 2023

Accepted: 4 October 2023

Published: 6 October 2023



**Copyright:** © 2023 by the authors. Licensee MDPI, Basel, Switzerland. This article is an open access article distributed under the terms and conditions of the Creative Commons Attribution (CC BY) license (<https://creativecommons.org/licenses/by/4.0/>).

## 1. Introduction

The sustainability of agricultural production depends, to a great extent, on the development of innovative technological solutions with a reduced impact on the environment which allow for the partial substitution of the use of agrochemicals and reduce the negative effects associated with their continued use [1]. Rice and wheat are two of the most important cereals worldwide. Both crops suffer from seed- and soil-borne diseases that require the extensive use of chemicals for seed treatment, and later, during growth, to prevent losses due to foliar and panicle diseases. The international trade of both grains is subjected to strict limits on agrochemical residues [2], which in turn results in a challenge to the farmers, who have fewer options to secure the health of their crops. In this sense, the development and potential application of biogenic nanoparticles that contribute to the control of phytopathogens and plant growth in crops is promising. Copper has been used in agriculture to control oomycetes, fungi, and bacteria for over a century, playing important roles in integrated pest management [3]. However, due to its accumulation in the

soil, innovative formulation technologies with reduced copper contents are necessary. One strategy to maximize its effectiveness is to reduce the particle size of the active substance to improve the coverage of treated surfaces. Small particles with high surface/volume ratios, such as copper nanoparticles, could represent an advantage by reducing the total amount of elemental copper needed to obtain the same effect [3]. However, the biogenic synthesis of copper nanoparticles has seldom been studied.

Nanometric-scale metal particles are widely studied due to their various applications, which are based on their physicochemical properties. These properties are conferred by their size and their surface and internal structures, and are different from particles of the same composition, but larger [4]. Among the potential advantages of metallic nanoparticles are their antifungal properties. For example, it was recently demonstrated that metallic nanoparticles could inhibit the growth of fungi that cause the biodeterioration of archaeological materials [5] or mycotoxin producers [6]. The adverse effects of different fungal strains are not only related to biodeterioration, but also to their negative impacts on human and animal health or on agriculture. In particular, the use of metallic nanoparticles in the agricultural area as an alternative to agrochemicals is very promising [7]. Recent works have demonstrated the potential use of nanoparticles in the control of phytopathogens and the promotion of plant growth, as well as nanosensors and nanoherbicides, with a high impact on agriculture [8–10]. Metal oxide nanoparticles and metal nanoparticles, due to their antimicrobial properties, have the ability to control and combat phytopathogens. Therefore, the application of nanoparticles of zinc oxide, titanium dioxide, copper, and silver for plant disease management is currently a major aspect of phytonanotechnology in agriculture [11].

Different methods of biological synthesis of nanoparticles, using plants, algae, fungi, and bacteria, have been reported as alternatives to physical and chemical methods, since the latter involve the use of toxic agents or agents posing potential environmental and biological risks [12]. For example, metabolites involved in the free-biomass filtrates of endophytic bacteria were used as biocatalysts for green synthesis of silver nanoparticles (AgNPs) [13] and copper nanoparticles [14]; both metallic nanoparticles showed promising activity in terms of controlling the phytopathogen growth. The main components which are involved in the production of nanoparticles using biological methods are a solvent medium, an environmentally friendly reducing agent, and a non-toxic stabilizing agent [15]. In particular, the extracellular synthesis from fungi has advantages, since they produce a large amount of proteins that can act as stabilizing agents (capping) on the surfaces of the nanoparticles. Moreover, as an extracellular synthesis, it facilitates the purification and scaling processes of the nanoparticles [16–18].

*Trichoderma* spp. has been widely used in agricultural applications due to its well-known biological control and plant growth promotion [19]. Although the extracellular synthesis of biogenic AgNPs by fungal strains isolated in Uruguay has been reported [20,21], *Trichoderma* spp. had not been included in that screening.

To the best of our knowledge, this is the first report of the evaluation of nanoparticles for the control of fungal phytopathogens from crops in Uruguay. To this end, our study aimed for the biosynthesis of AgNPs and copper oxide nanoparticles (CuONPs) using a strain of *T. harzianum* as a green, eco-friendly, and biocompatible method. The nanoparticles were purified and characterized. Then, the *in vitro* antifungal activity of the nanoparticles against pathogens of rice and wheat from Uruguay, as well as their effect on seed germination, were evaluated.

## 2. Materials and Methods

### 2.1. Organisms

Strains of *Trichoderma harzianum* TA2 (ILB395), *Rhizoctonia oryzae-sativae* (ILB 428), *Sclerotium oryzae* (ILB 425), *Pyricularia oryzae* (Po290), and *Fusarium graminearum* (02020) were provided by S. Lupo (UDELAR, Montevideo, Uruguay), S. Martínez (INIA, Montevideo, Uruguay), and S. Pereyra (INIA, Uruguay), respectively, to be used in the present study.

The phytopathogen microorganisms used in the antifungal evaluation had previously been isolated from rice and wheat crops in Uruguay.

## 2.2. Biological Synthesis and Purification of Metallic Nanoparticles

A strain of *Trichoderma harzianum*, TA2, was used for the nanoparticle biosynthesis. The mycelia were grown on potato dextrose agar (PDA, BD Difco) at 28 °C, and two plugs 0.9 cm in diameter were then transferred to 250 mL flasks containing 100 mL potato dextrose broth (PDB, BD Difco). Fungal growth was carried out at 28 °C, with agitation on an orbital shaker operating at 150 rpm for 72 h. The biomass from the cultures was harvested by filtration, then washed extensively with sterilized distilled water to remove any remaining media components.

The synthesis of the AgNPs was carried out as described by Sanguiñedo et al. [20]. Wet fungal mycelia were suspended in sterilized distilled water (0.1 g/mL) and incubated with agitation on an orbital shaker operating at 150 rpm. Then, the cell-free filtrate was collected by filtration of this suspension through a membrane filter with 0.45 µm pore size. Finally, 50 mL of the cell-free filtrate was added to 50 mL of a silver nitrate solution (1, 5, and 10 mM AgNO<sub>3</sub>). The mixture was incubated in dark. Furthermore, different pH conditions (pH 5, 6, 7, and 9) were evaluated. The synthesis of CuONPs was carried out according to the same general methodology, but replacing AgNO<sub>3</sub> with 5 mM CuCl<sub>2</sub>, at different pH conditions (5, 7 and 9) in the synthesis reaction, as reported by Cuevas et al. [22]. The absorbance spectrum was measured in the range of 250–800 nm at different times. The remaining cell-free filtrate was used as the control. When there was no increase in the maximum absorption peak of metallic nanoparticles, the samples were centrifuged at 11,140 g for 10 min. The supernatant was removed, and the nanoparticles (NPs) were washed twice using sterilized distilled water by centrifuging the resuspended nanoparticles for 5 min at 11,140 g. The absorbance peak of the purified nanoparticles was measured and the concentration was estimated according to Paramelle et al. [23].

## 2.3. Characterization of Nanoparticles

### 2.3.1. UV-Vis Spectroscopy

The absorbance spectrum was measured using a UV/Visible spectrophotometer, model 6715, JENWAY (England), in the range of 250–800 nm in order to monitor the formation of nanoparticles evidenced for surface plasmon resonance (SPR) bands of the metal NPs.

### 2.3.2. Scanning Electron Microscopy (SEM) and High Resolution Transmission Microscopy (HR-TEM)–Energy Dispersive Spectroscopy (EDS)

For the SEM analysis, a volume of 10 µL of aqueous solution (0.1 mg/mL) of NPs was placed onto a grid and allowed to dry at room temperature. The SEM analysis was performed using a JEOL JSM-5900LV electron microscope. For the HR-TEM analysis, the samples in ethanol 95 were completely dried, and then observed with a JEOL JEM 2100 electron microscope with 200 kV acceleration voltage using a copper or nickel grid for AgNPs and CuONPs, respectively. In addition, the elemental chemical composition was studied with an X-ray EDS probe on the surfaces of the NPs. Then, the sizes of the NPs were determined by image analysis using ImageJ Software.

### 2.3.3. Dynamic Light Scattering (DLS) and ζ-Potential

The hydrodynamic diameter was determined and the ζ-potential of the NPs was measured. Samples were prepared at pH 6 in Milli-Q water. For DLS determination, each sample was measured at 25 °C 3 times, combining 5 runs per measurement. In the case of ζ-potential, each sample was measured at 25 °C 3 times, combining 10 runs per measurement. The results were treated using the Malvern software Zetasizer.

#### 2.3.4. Confocal Raman Microscopy (CRM)

An aliquot of NPs was deposited onto an aluminum support and dried at room temperature for analysis by CRM. The laser power was carefully calibrated to avoid decomposition. Subsequently, the samples were examined, resulting in confocal Raman images of  $40 \times 40 \mu\text{m}$ , processed using a  $40 \times 40$  point grid. Measurements were performed on the Alpha 300 RA WITec Raman Microscope using a 532 nm excitation laser focused through a  $100\times$  objective.

#### 2.4. Antifungal Activity

The minimum inhibitory concentration (MIC) of NPs was determined using the microdilution technique [24]. Suspensions of the microorganisms ( $1 \times 10^4$  spores/mL) were seeded in RPMI broth with serial dilutions of the NP solution (in water). As controls, the culture broth and sterile water (same volume as the NP solution) with and without the suspension of the microorganism were seeded. After incubation for 96 h at  $28^\circ\text{C}$ , the minimum concentration that caused visible inhibition of the microbial growth was determined. All experiments were carried out in triplicate, and the results were indicated as the modal value when distinct values were found, as reported by Melhem et al. [25]. The activity was carried out against the pathogenic fungi *Fusarium graminearum* and *Pyricularia oryzae*. In the MIC assays, 5mM  $\text{AgNO}_3$  and 5 mM  $\text{CuCl}_2$  were used as controls.

Furthermore, the effects of NPs on the mycelium growth of non-sporulated phytopathogens *Sclerotium oryzae* and *Rhizoctonia oryzae-sativae* were evaluated, as previously reported [26]. Agar blocks (plugs) of fresh mycelium were punched out from the edge of the fungal colony using a sterile punch 5 mm in diameter. The plates were inoculated in the center with one plug per plate; they contained PDA supplemented with 1 mL of four different concentrations (two-fold dilutions) of NPs ( $\leq 0.14 \mu\text{M}$  AgNPs and  $50 \mu\text{M}$  CuONPs). They were incubated for 5 days at  $28^\circ\text{C}$ . Control cultures of fungal strains grown in PDA were also included. After that period, the diameter of the mycelium was measured and compared with the control. The diameter of the mycelial growth in PDA medium (without nanoparticles) served as the control, representing the 100% growth (0% inhibition). The inhibition caused by each nanoparticle concentration was expressed as a percentage, comparing the fungal growth with the control.

#### 2.5. Seed Germination Toxicity Test

Rice (*Oriza sativa*) and wheat (*Triticum aestivum*) seeds from the commercial cultivars INIA Tacuarí and INIA Genesis 4.33, respectively, were soaked in distilled water for 10 min to soften the seeds' coats and initiate the process of germination. In order to rule out a negative effect on seed germination and to evaluate the effect on seed-borne fungal growth, seeds were soaked in NPs solutions ( $0.14 \times 10^{-9}$  M AgNPs and  $50 \mu\text{M}$  CuONPs) for 2 h, based on Spagnoletti et al. [27]. Germination was assessed on three plates with PDA, each one containing 10 seeds, and this was repeated independently at least 3 times. Seeds treated with 5 mL distilled water, with 5 mL of a solution of 5 mM  $\text{AgNO}_3$  or 5 mL of 5 mM  $\text{CuCl}_2$ , were set as controls. Petri dishes were incubated at  $25^\circ\text{C}$  for 6 days. Seeds with coleoptiles and roots longer than 2 mm were scored as positive for the test [27].

#### 2.6. Statistical Analysis

The experiments were performed at least in triplicate, and averages and standard deviations were calculated for all experiments. The results are plotted as mean values with bars that represent standard deviations. The data were statistically analyzed using the generalized linear model, assuming a binomial distribution and using the logit function. The treatments were compared using the DGC test [28], with a significance level of 0.05. For these analyses, the InfoStat software (InfoStat Group, FCA, National University of Córdoba, Córdoba, Argentina) was used.

### 3. Results

#### 3.1. Biological Synthesis of Metallic Nanoparticles

After the AgNPs' synthesis reaction with the fungal filtrate began, a band in the UV-vis spectrum was observed at 440 nm, corresponding to the SPR band of the AgNPs (Figure 1a). A higher absorbance level of SPR correlates with more efficient synthesis. Therefore, better production of AgNPs was observed using 5 and 10 mM AgNO<sub>3</sub> rather than 1 mM. Furthermore, the spectrum showed a broad band from 250–350 nm, which corresponded to components of the extracellular extract of the fungus. Furthermore, at different pH levels, the UV-vis spectra were very similar, showing SPR bands at 440 nm of the AgNPs (Figure 1b).

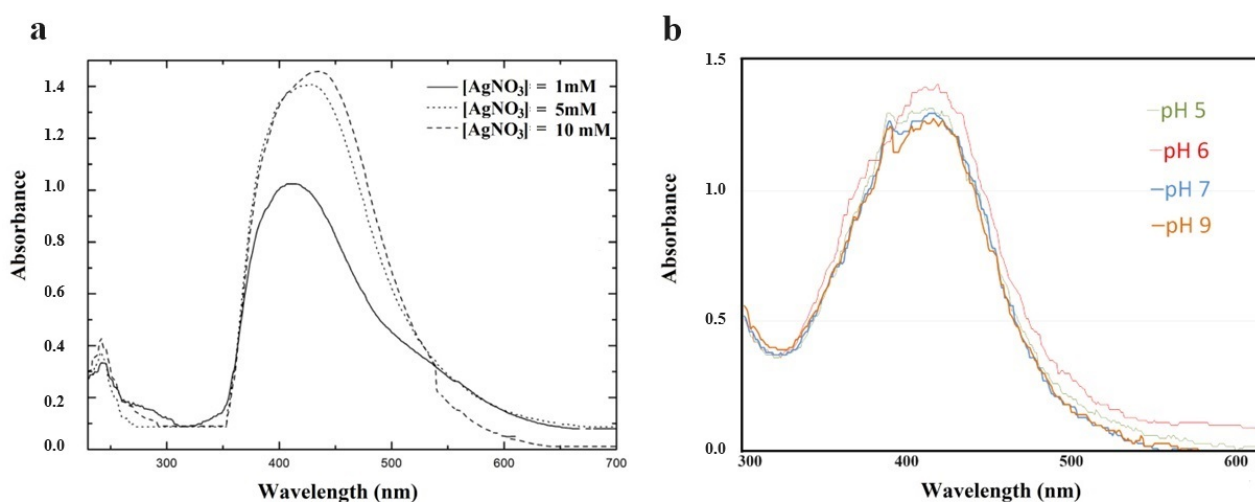


**Figure 1.** UV-vis spectra of AgNPs. (a) Synthesis reactions at different AgNO<sub>3</sub> concentrations, showing the SPR band at 440 nm. (b) SPR at different pH levels.

Then, the synthesis of CuNPs was carried out, replacing AgNO<sub>3</sub> with CuCl<sub>2</sub>. The UV-Vis spectrum showed a band at 390 nm, corresponding to the SPR attributed to CuONPs (Figure 2a). In addition, the effect of pH variation on the synthesis reaction was studied. Figure 2b shows the spectra in different conditions, and the peak corresponds to the CuONPs. From these results, it was concluded that at pH = 7, the synthesis was favored, showing the highest band at 390 nm, followed by pH = 9 and pH = 5.

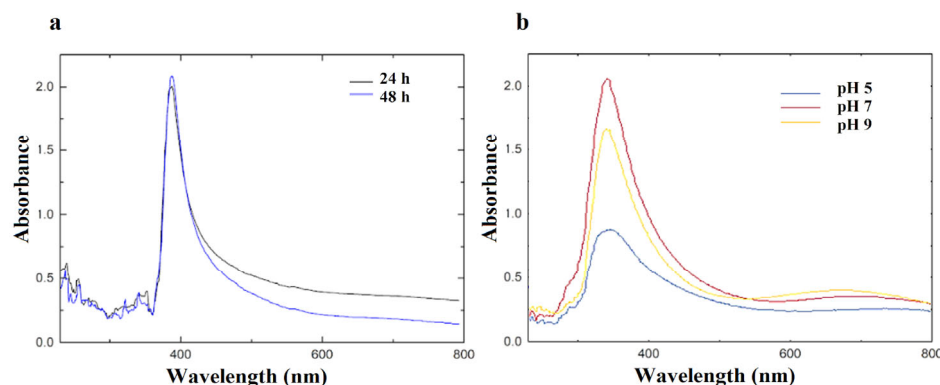


**Figure 2.** UV-vis spectra for CuNP synthesis. (a) After 24 and 48 h of reaction. (b) Reactions at different pH.

After synthesis, both AgNPs and CuNPs were purified. For this purpose, they were centrifuged, washed (to remove excess extract and reagents), and resuspended in water. The purified nanoparticles were stable to this process, showing SPR bands at 440 and 390 nm for AgNPs and CuONPs, respectively, in the UV-vis spectra.

Both AgNPs and CuONPs showed colloidal stability over six months, maintaining their characteristic SPR bands in the UV-vis spectra throughout that time. The nanoparticles were stored in distilled water at room temperature.

### 3.2. Characterization

#### 3.2.1. SEM and HR-TEM-EDS

In the first instance, SEM was performed, showing mainly spherical nanoparticles in all of the studied samples (Figure 3a,b). Then, the sizes of the nanoparticles were determined by HR-TEM and DLS analysis. The average size of the NPs, according to transmission electron microscopy (TEM), was  $8 \pm 2$  nm and  $3.5 \pm 0.5$  nm for AgNPs and CuONPs, respectively. In addition, the characterization by DLS showed a larger average size ( $17.5 \pm 1.1$  nm and  $26.4 \pm 2.2$ ), which was expected, since the DLS measures the hydrodynamic diameter of the particles. Both nanoparticles showed a slightly polydisperse distribution ( $<0.4$ ).

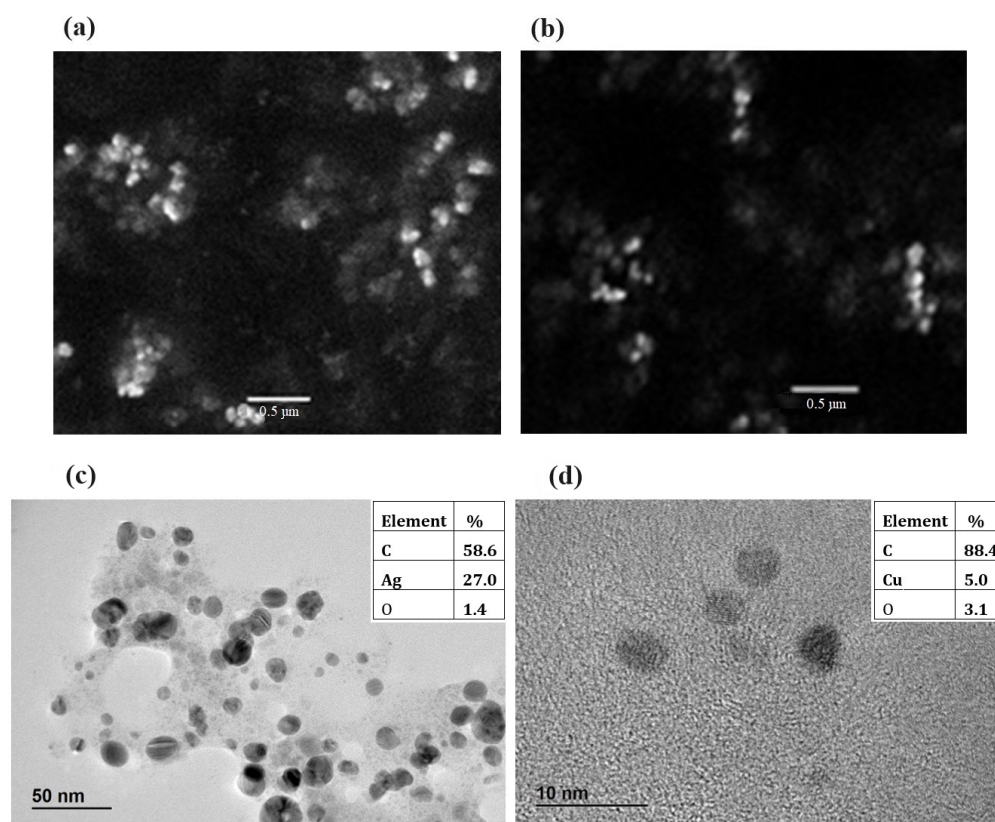


**Figure 3.** Analysis of AgNPs and CuONPs by electron microscopy. (a,b) SEM and (c,d) HR-TEM (EDS) analyses of biogenic nanoparticles. (a,c) AgNPs; (b,d) CuONPs.

The results of the elemental analysis of the nanoparticles by EDS showed Ag and Cu among the principal elemental components of AgNPs and CuONPs, respectively (Figure 3c,d).

#### 3.2.2. DLS and $\zeta$ -Potential

The size characterization DLS showed a single population with a hydrodynamic diameter of  $17.5 \pm 1.1$  nm and a polydispersity index (PDI) of 0.211, and  $26.4 \pm 2.2$  nm, PDI 0.302, for AgNPs and CuONPs, respectively (Figure 4a,b). Both NPs showed slightly polydisperse distributions (PDI  $< 0.4$ ).

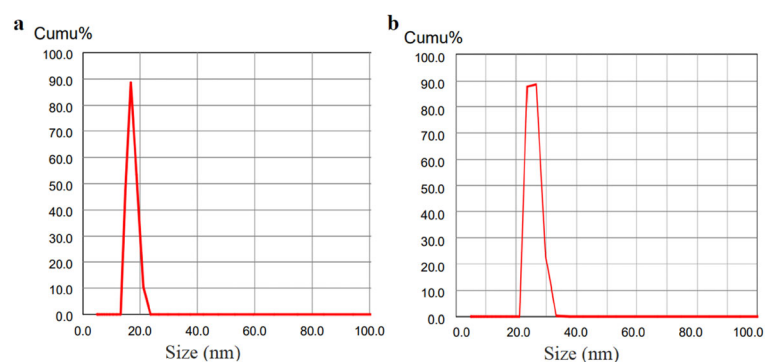


Figure 4. DLS measurements of AgNPs (a) and CuONPs (b) in solution.

Measurements of the  $\zeta$ -potential showed that AgNPs had a net negative surface charge,  $-21.5 \pm 6.0$  mV (Figure 5a). Similarly, CuONPs showed a net negative surface charge of  $-13.9 \pm 4.9$  mV (Figure 5b).

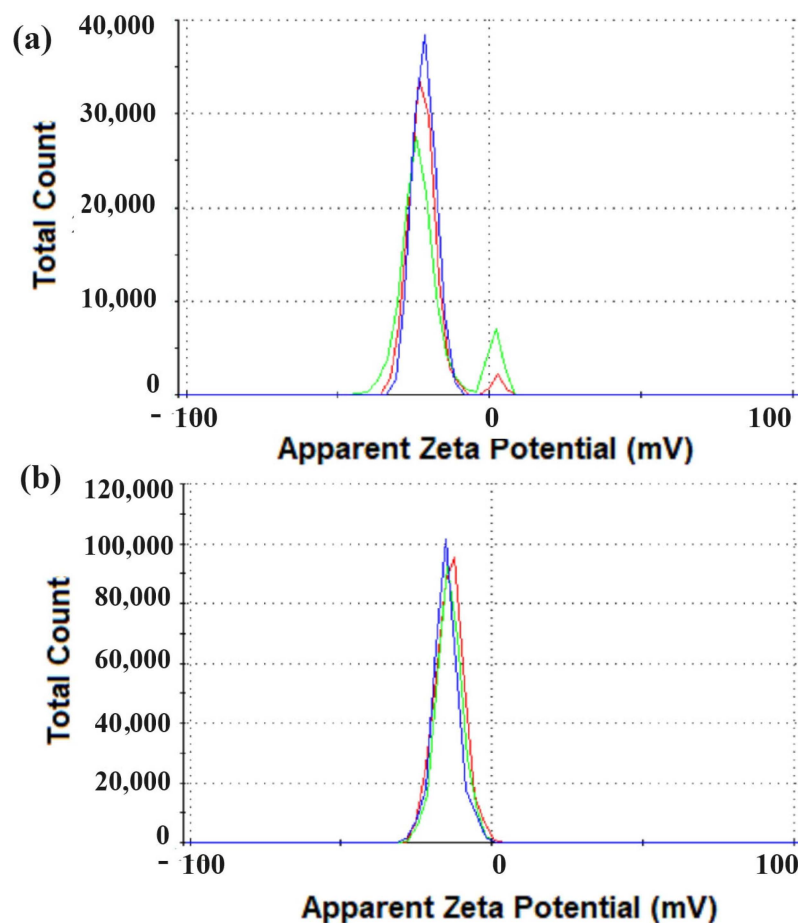
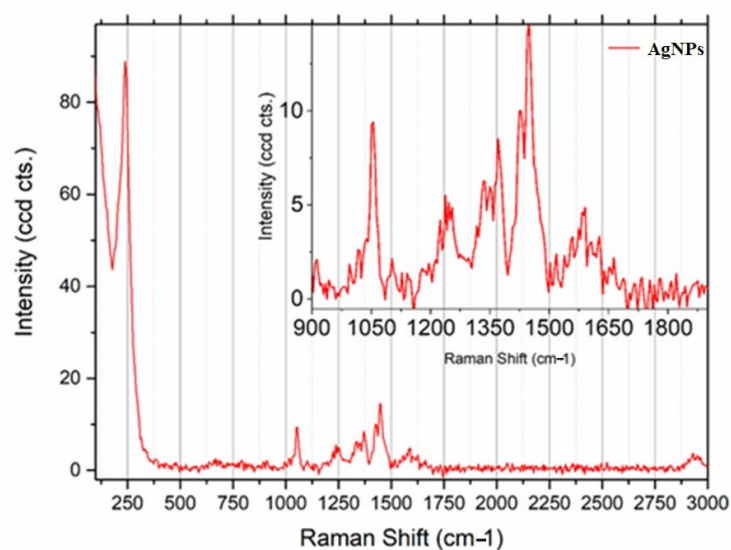


Figure 5.  $\zeta$ -potential measurements of AgNPs (a) and CuONPs (b) in solution.

### 3.2.3. Confocal Raman Microscopy

In order to obtain information on the nature of the functional groups on the nanoparticle surfaces (capping), an analysis was carried out using CRM. As shown in Figure 6, the bands observed in the region between  $900$  and  $1700$   $\text{cm}^{-1}$  (1042, 1240, 1331, 1360, 1437, 1572) can be attributed to the presence of the amino acids l-alanine, l-glutamate, and l-proline [29]. Furthermore, the presence of the band at  $230$   $\text{cm}^{-1}$  can be attributed to the Ag-N stretching mode, indicating that the nitrogen atoms from the fungal extract are part of the capping of these nanoparticles (Figure 6).



**Figure 6.** Raman spectra from CRM for AgNPs at 532 nm.

Furthermore, the CRM results affirmed the existence of CuO nanoparticles. A hyperspectral image of  $40 \times 40 \mu\text{m}$  was processed in a grid of  $40 \times 40$  points, then analyzed using True Components in WITec Project 5 Plus [30]. As can be observed in Figure 7, two main regions could be distinguished in the sample, Zone 1 and Zone 2, after multivariate hyperspectral analysis. Zone 1 and Zone 2 correspond to regions with low and high concentrations of CuO nanoparticles, since the peaks associated with it could be confirmed by the following Raman shift positions: 282, 325, and  $606 \text{ cm}^{-1}$  [14,31]. In the case of a region with a low concentration of CuO nanoparticles, the observed bands were mainly located at: 1285, 1362, 1441, 1502, 1580, and  $1615 \text{ cm}^{-1}$ , and they could be attributed to several amino acids, such as l-valine, l-serine, and l-tryptophan [29]. While spectra typically exhibit similarities, a closer examination revealed that the bands in the range of  $700$  to  $1800 \text{ cm}^{-1}$  underwent alterations, including shifts in wavenumber and alterations in intensity. These changes may result from the impact of the presence of nanoparticles and their proximity interactions with the biological sample. Furthermore, the nanoparticles may cause signal enhancement, resulting in comparatively greater intensity variations.

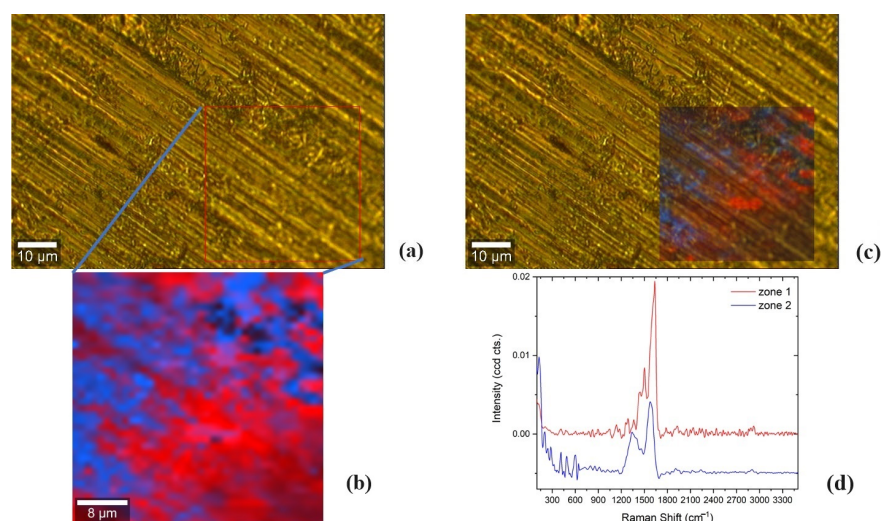


**Figure 7.** Analysis of CuONPs by CRM. (a) Optical image and (b) confocal Raman images indicating low- and high-concentration regions of CuO nanoparticles (Zone1 and Zone2). (c) Overlay of CRM image over optical image. (d) Raman spectra corresponding to Zone 1 and Zone 2.

### 3.3. Antifungal Activity

We determined the MIC of nanoparticles against *Fusarium graminearum* and *Pyricularia oryzae*. For this standardized method, spore suspensions of filamentous fungi were used as the inoculum for broth culture. Then, the MIC was defined as the minimum concentration that would cause visible inhibition of fungal growth; at concentrations below the MIC, as well as in the growth controls (without antifungal), the spores germinated and mycelium growth was observed. Growth inhibition of *Fusarium graminearum* was observed by AgNPs and CuONPs. Furthermore, AgNPs also inhibited the growth of *Pyricularia oryzae*. Likewise, it is important to highlight that the inhibition concentrations of AgNPs and CuONPs were lower than AgNO<sub>3</sub> and CuCl<sub>2</sub>, respectively (Table 1, Figure S1).

**Table 1.** MIC results obtained against *F. graminearum* and *P. oryzae*.

	MIC * (μM)	
	<i>F. graminearum</i>	<i>P. oryzae</i>
AgNPs	$34 \times 10^{-6}$	$34 \times 10^{-6}$
AgNO <sub>3</sub>	78	78
CuONPs	NI	6.3
CuCl <sub>2</sub>	NI	NI

NI: No inhibition. \* Results are indicated as the modal values if distinct values were found.

The antifungal activity of NPs on the non-sporulated rice pathogens *Rhizoctonia oryzae-sativae* and *Sclerotium oryzae* was also evaluated. For these purpose, different nanoparticle concentrations were incorporated into the solid medium, and a plug of fresh mycelium was used as the inoculum. The diameter of the mycelial growth on the PDA medium (without nanoparticles) served as the control, representing 100% growth (0% inhibition). The inhibition caused by each nanoparticle concentration was expressed as a percentage, comparing the fungal growth with the control, as explained in the Section 2. The nanoparticles showed inhibition of the mycelial growth (Table 2, Figure S2). AgNPs (0.14 ηM) produced 13% inhibition of *R. oryzae-sativae* and 19% inhibition of *S. oryzae*. Furthermore, CuONPs (50 μM) produced 22% inhibition of the growth of *R. oryzae-sativae* and 5% inhibition of *S. oryzae*. Otherwise, no fungal growth inhibition was observed at AgNO<sub>3</sub> or CuCl<sub>2</sub> concentrations less than 0.12 mM.

**Table 2.** Antifungal activity of AgNPs and CuONPs against *R. oryzae-sativae* and *S. oryzae*.

	% Inhibition	
	<i>R. oryzae-sativae</i>	<i>S. oryzae</i>
AgNPs	11 ± 1	19 ± 3
CuONPs	22 ± 4	5 ± 2

### 3.4. Seed Germination Toxicity Test

The purpose of this test was to verify that the nanoparticles did not negatively affect the germination of wheat and rice seeds, and to evaluate the effect on seed-borne fungal growth. The treatment with AgNO<sub>3</sub> (5 mM) slowed down the germination of wheat seeds at 3 days of incubation (Figure 8a). However, wheat seeds treated with AgNPs (55 pM) showed germination and development of radicles that were similar to control seeds. Furthermore, AgNO<sub>3</sub> and AgNPs showed total and partial inhibition of the microbial growth, respectively, compared with the control. Although, after 6 days of incubation, no significant differences in germination were found among the treatments ( $p > 0.05$ ), a tendency towards higher germination of wheat seeds treated with AgNPs compared to the control and to AgNO<sub>3</sub> was observed (Figure 8b).

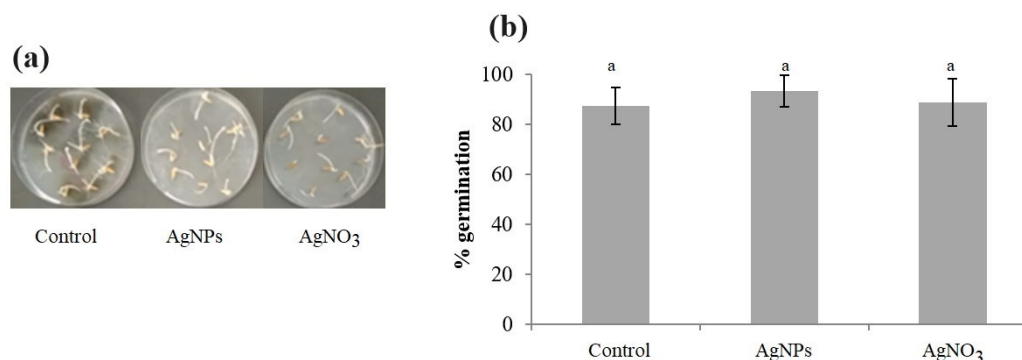


**Figure 8.** Germination of wheat seeds. (a) Plate germination assay. (b) Germination percentage. Different letters indicate significant differences ( $p < 0.05$ ).

In the evaluation on rice seeds treated with AgNPs, no differences were observed in germination or microbial growth compared to the control (Figure 9a). Although AgNO<sub>3</sub> slowed down the germination of seeds and produced an almost total inhibition of microbial growth, no significant differences in germination were detected at 3 or 6 days of incubation (Figure 9b).

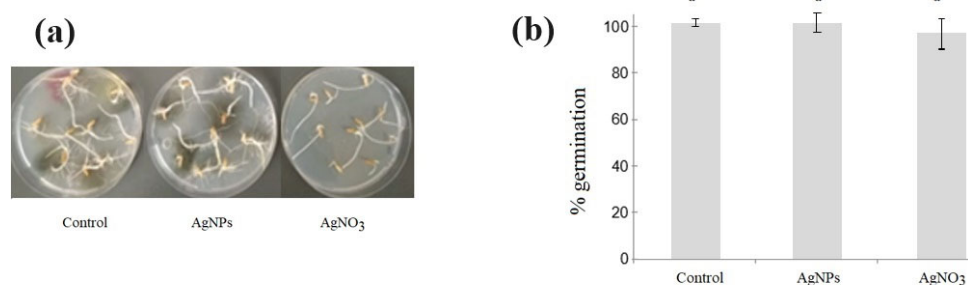


**Figure 9.** Germination of rice seeds. (a) Plate germination assay. (b) Germination percentage. Different letters indicate significant differences ( $p < 0.05$ ).

The treatment of wheat and rice seeds with CuONPs (0.2 mM) and CuCl<sub>2</sub> (5 mM) was also evaluated, but no differences were observed in germination or microbial growth compared with the control (Table 3).

**Table 3.** Germination of wheat and rice seeds.

	% Germination Wheat Seeds	Rice Seeds
Control	78 ± 8 <sup>a</sup>	98 ± 4 <sup>a</sup>
CuONPs	83 ± 10 <sup>a</sup>	98 ± 4 <sup>a</sup>
CuCl <sub>2</sub>	84 ± 8 <sup>a</sup>	96 ± 5 <sup>a</sup>

Different letters indicate significant differences ( $p < 0.05$ ).

#### 4. Discussion

The application of nanoparticles in agriculture is a novel approach that has proven very effective against plant pathogens. For example, greenhouse and field trials have shown that AgNPs-based formulations are equally or more efficient than copper-based antimicrobial compounds used in agriculture to reduce bacterial and fungal diseases in tomato and citrus [32]. While metal NPs could be considered as a novel tool to be used for the more sustainable management of agricultural diseases and pests, it is also important to develop methods for their production that are sustainable. Contrary to their chemical synthesis, the biological synthesis of metal NPs is envisaged as a sustainable method [33]. It has been suggested that fungi could be a safer choice for large-scale nanoparticle production, because

they are simple to deal with in downstream processing and secrete a significant number of enzymes for the redox reactions [34]. The approaches to extracellular biosynthesis by fungi show that the bioactive metabolites produced would be responsible for the reduction of the metal, and it is expected that the same mechanism could be involved in both  $\text{Ag}^+$  and  $\text{Cu}^{2+}$  reduction for nanoparticle synthesis [35]. Considering this, AgNPs and CuONPs were synthesized from *Trichoderma harzianum* TA2 fungus. AgNPs' production and potential uses in agriculture have been studied with promissory results [36,37]. However, it is necessary to generate a greater number of studies on the mycosynthesis of copper NPs for a better understanding of the mechanisms of action and production, considering their potential application [38]. Because copper is usually applied as a fungicide in different forms in agriculture, it was interesting to explore the production and potential uses of copper NPs in addition to biogenic AgNPs.

UV-vis spectra of biogenic AgNPs showed bands close to 250–300 nm, which could correspond to different components of the extracellular extract of the fungi [4]. The band close to 250 nm (Figure 1) could be attributed to electronic excitation in tryptophan and tyrosine residues in proteins, as previously reported for biogenic nanoparticles from *Trichoderma viride* [39]. As expected from previous studies [20], the peak corresponding to the SPR of the AgNPs was found at 440 nm. Different concentrations (1 mM, 5 mM, and 10 mM) of  $\text{AgNO}_3$  were evaluated, according to previous reports regarding the synthesis of other fungal nanoparticles [40]. Based on the results, 5 mM  $\text{AgNO}_3$  was selected for all subsequent biosynthesis processes with *Trichoderma harzianum* TA2. Furthermore, the SPR bands of AgNPs did not show significant differences in different pH conditions. In addition, the synthesis of copper NPs was evaluated based on reports by Cuevas et al. [22]. This type of synthesis has been studied less than that of other metallic nanoparticles, such as gold and silver. As reported in the literature [22,41], copper NPs show more variable composition and properties. Under the evaluated conditions, the synthesis carried out with *T. harzianum* TA2 showed a band in the spectrum that suggests the formation of CuONPs. As shown in Figure 2a, the band corresponding to the SPR was found at 390 nm, which could be attributed, as reported in the literature [41], to CuONPs.

For the biogenic synthesis of CuONPs, previous studies have reported bands at different wavelengths in the UV-vis monitoring, attributing them to copper or copper oxide nanoparticles. Likewise, it has been reported that the pH could produce shifts in the bands obtained in the UV-vis spectrum of CuONPs [22]. Taking this into account, in this work, the results obtained for the synthesis of CuONPs at different pH levels are reported. Although, at pH 5, no shift was observed in the UV-vis spectrum, a decrease in the band at 390 nm was observed. Moreover, at pH 9, a small, broad peak between 600 and 800 nm was observed. A similar broad band was previously observed in the UV-visible spectra of biosynthesized copper nanoparticles at pH 9.0 and 5 mM of  $\text{CuCl}_2$ ; these red shifts in absorption between 590 and 800 nm were attributed to the characteristic absorption peaks of cuprous oxide ( $\text{Cu}_2\text{O}$ ) nanoparticles [22].

Both AgNPs and CuNPs synthesized with *Trichoderma harzianum* TA2 extracts were stable after their purification by centrifugation. Similarly, stable purified nanoparticles have previously been reported [20]; the biogenic metallic nanoparticles were synthesized using fungi isolated from fruits and wood in Uruguay, such as *Penicillium expansum*, *Punctularia atropurpurascens*, and *Phanerochaete chysosporium*. The SEM and HR-TEM images showed spherical nanoparticles for both NPs. Furthermore, the nanoparticle sizes were determined by HR-TEM and DLS analysis. The nanoparticles were small in size (less than 10 nm in diameter by HR-TEM). In addition, the characterization by DLS showed a larger average size. This is expected, since the DLS measures hydrodynamic size, which is the size of the nanoparticle, including the capping agent plus the liquid layer around the particle. However, for HR-TEM analysis, the nanoparticles were completely dried, and the micrographs mostly show the metallic cores of the nanoparticles. It has been reported that, in conventional TEM, the sample is exposed to high vacuum while on the grid, and the corona collapses into a desiccated layer, which causes particles to appear

smaller than the DLS-measured hydrodynamic sizes [42–44]. Both nanoparticles showed slightly polydisperse distributions ( $<0.4$ ) consistent with previous reports on other biogenic nanoparticles from fungi [20].  $\zeta$ -potential measurements showed the colloidal stability of the nanoparticles; nanoparticles with a net potential close to zero will probably aggregate, losing their properties as nanomaterials [45]. In this work, the electrostatic repulsive forces between the negative surface charges of AgNPs and CuONPs probably played an important role in their stability.

The results of the nanoparticles elemental analysis by EDS were consistent with the biogenic synthesis conditions carried out, showing silver and copper among the principal chemical elemental components. The presence of C can be attributed to the scattering of capping agents in the biogenic synthesis, as reported by Fouada et al. [14]. Furthermore, the high percentage of oxygen present could be attributed not only to the presence of CuONPs, but also to the capping agent of the biogenic nanoparticles. This result would be consistent with the SPR band obtained near 390 nm, as was reported for the biogenic synthesis of CuONPs [41]. Additionally, in order to confirm the presence of CuO nanoparticles, we proceeded with confocal Raman imaging. The CRM results affirmed the existence of CuO nanoparticles. The obtained data were in agreement with various spectroscopic studies (Raman and FTIR) that confirmed that the peak of the CuO-NPs was in the range of  $400\text{--}700\text{ cm}^{-1}$  [14,31].

The surface functional groups and capping of the NPs were also characterized by CRM, indicating that the biological synthesis produces metallic nanoparticles coordinated with N coming from the fungal protein. In addition, as previously reported, the presence of the Raman bands positioned at the fingerprint region between  $900$  and  $1700\text{ cm}^{-1}$  can be attributed to the presence of amino acids, suggesting that proteins from the fungal extract are part of the capping [46].

The biogenic synthesis of AgNPs using a commercial powder of *Trichoderma harzianum* was previously reported [47]. Coincident with this work, the presence of peaks corresponding to proteins and amino acid residues in the UV-vis spectra of biogenic nanoparticles indicated they were involved in the formation and stabilization of the nanoparticles. Furthermore, it was demonstrated that the capped, but not the uncapped, biogenic nanoparticles showed biological activity in the control of the phytopathogen *Sclerotinia sclerotiorum* [47]. Additionally, some works regarding *T. harzianum* AgNPs with antibacterial, larvicidal, and pupicidal activities were reported [48–51].

Metallic nanoparticle synthesis by *Trichoderma* spp. was recently reviewed [37]. Copper biogenic nanoparticles from *T. asperellum*, *T. atroviride*, and *T. koningiopsis* were reported. *T. atroviride* copper nanoparticles were able to inhibit the phytopathogens *Poria hypolateritia*, causing red root rot, and *Phomopsis theae*, causing Phomopsis canker diseases. In the present work, the antifungal activity of AgNPs and CuONPs against wheat and rice pathogens was evaluated in vitro, showing promising results. The MIC values were lower than AgNO<sub>3</sub> or CuCl<sub>2</sub> solution, respectively, against *Fusarium graminearum* and *Pyricularia oryzae*. Similar MIC differences between AgNPs and AgNO<sub>3</sub> have previously been reported [44]. Furthermore, copper nanoparticles are more effective against plant pathogens than the copper-based antimicrobial compounds used in agriculture, which contain micron-sized insoluble metallic copper compounds. Nanoparticles have unique physical and chemical properties, and their smaller size and higher surface-to-volume ratio allow metallic particles to penetrate microbial membranes and release metal ions into solution more efficiently, conferring higher antimicrobial activity compared with the micron-sized formulations [32]. For example, it was reported that 100 mM copper salt solutions did not show any significant activity against three strains of *Fusarium* spp. [52]. In another recent work, although the 60 mM copper solution showed antifungal activity against phytopathogens, copper nanoparticles showed higher activity at lower concentrations [53].

Additionally, although the antimicrobial properties of nanoparticles depend on size, shape, charge, chemical composition, and morphology, it has been reported that AgNPs are able to inhibit microbial growth more actively than copper nanoparticles [54]. Further-

more, inhibition growth of *R. oryzae-sativae* and *S. oryzae* mycelia was observed in media supplemented with AgNPs and CuONPs.

In recent years, research regarding the possible applications of nanotechnology in agriculture has gained more relevance due to its promising potential to increase the efficiency of agricultural inputs and to offer alternative solutions to current problems. These applications include the use of nanomaterials as nanofertilizers, nanobiosensors, nano-enabled remediators of contaminated soils, and nanopesticides, due to their antifungal properties [55]. The potential of NPs in the control of phytopathogens has been reported, as they becoming potential candidates for use in agriculture as a sustainable alternative to commonly used chemical pesticides for disease control [56]. Mishra et al. [36] synthesized biogenic AgNPs from bacteria *Serratia* sp. BHU-S4 with in vitro antifungal activity against *Bipolaris sorokiana*, which is responsible for leaf spot disease in cereals. These results had a positive impact on the growth of the wheat plants when treated with AgNPs in a greenhouse experiment.

Seeds are the most basic means of production in agriculture, forestry, and horticulture. Currently, the management practices for commercial farms include seed treatment with different chemical fungicides, such as prothioconazole and tebuconazole for rice seeds in Uruguay [57]. Unfortunately, the evolution of fungicide resistance has become a major issue, and it is important to monitor the sensitivity of fungicides against phytopathogens. For example, Ranagarani et al. [58] demonstrated the efficacy (inhibition percentage) of different fungicides used in rice to inhibit *S. oryzae* at 0.5–3.0 g/L concentrations. Furthermore, there is an urgent need for new antifungal treatments. The possibility of offering a treatment of simple application to the producer and using lower concentrations of commercial pesticides is promising. Before any nanopesticides become available in agriculture, possible specific risks for plants, health, and the environment should be evaluated [32].

Increasing the germination percentage and emergence rate of seeds, as well as increasing protection against biotic stresses, is of extreme importance for agricultural purposes. To take advantage of the positive effects of nanotechnology being included in agronomic practices, the possible stress and toxicity that these metallic nanoparticles could cause in plants should be analyzed thoroughly. In this sense, the study of the impact of nanoparticles on seed germination is relevant as an indicator of toxicity [27]. In this work, the germination percentage of rice and wheat seeds treated with nanoparticles was evaluated to verify that the nanoparticles did not negatively affect germination. The results showed that the application of AgNPs and CuONPs did not have any negative effect on seed germination. Future works will include the evaluation of treated seeds in pot trials.

To our knowledge, this is the first report of the evaluation of nanoparticles for the control of fungal phytopathogens from crops in Uruguay. It is important to highlight that the production of both AgNPs and CuONPs from the same strain of *T. harzianum* was possible. Although the antimicrobial activity of nanoparticles against phytopathogens has previously been demonstrated [16], this is the first report of biogenic silver and copper oxide nanoparticles from a single strain of *T. harzianum* with antifungal activity against *R. oryzae-sativae*, *S. oryzae*, *P. oryzae*, and *F. graminearum*, phytopathogens of interest in Uruguay. Furthermore, the synthesis of the biogenic nanoparticles was faster and more efficient than previous reports using other fungi [20].

## 5. Conclusions

The current study revealed that it is possible to synthesize silver and copper biogenic nanoparticles from *Trichoderma harzianum* TA2. These nanoparticles were characterized by different methods, which provided information about their shape, size, superficial charge and capping nature. In addition, nanoparticles showed colloidal stability over time. For these reasons and due to the in vitro antifungal activity results, they are promising candidates for the control of phytopathogens affecting important and extensive crops. The biogenic metallic nanoparticles synthesized in this work could be a novel strategy and a biotechnological alternative contributing to integrated disease management in wheat and

rice crops. Future studies regarding the environmental impact and the in situ antifungal effect of using biogenic nanoparticles on the control of wheat and rice diseases caused by *P. oryzae*, *R. oryzae-sativae*, *S. oryzae*, and *F. graminearum* should be encouraged.

**Supplementary Materials:** The following supporting information can be downloaded at: <https://www.mdpi.com/article/10.3390/chemistry5040143/s1>. Figure S1: Determination of Minimum Inhibitory Concentration (MIC) against *Pyricularia.oryzae*. SC: sterile control. GC: growth control. Figure S2. Antifungal activity of AgNPs against *R. oryzae sativae* (% inhibition growth). GC: growth control (PDA). AgNPs: PDA supplemented with AgNPs.

**Author Contributions:** Conceptualization: S.A.; data curation: P.S. and R.F.; formal analysis: P.S.; methodology: P.S.; funding acquisition: S.A. and E.A.; supervision: S.A. and E.A.; resources: S.A., E.A. and R.F.; writing—original draft: P.S. and S.A.; writing—review and editing: S.A., E.A., R.F. and P.S. All authors have read and agreed to the published version of the manuscript.

**Funding:** This research was funded by Project INNOVAGRO FSA\_1\_2018\_1\_152546 (Agencia Nacional de Investigación e Innovación-Instituto Nacional de Investigación Agropecuaria), Posgrado en Biotecnología y Comisión Académica de Posgrado (CAP) (Universidad de la República, Uruguay), Program for the Development of Basic Sciences (PEDECIBA-Química) and Sociedad Uruguaya de Microbiología (SUM).

**Data Availability Statement:** The datasets generated and/or analyzed in the current study are available from the corresponding author upon reasonable request.

**Acknowledgments:** The authors acknowledge Sebastian Martínez, Sandra Lupo, and Silvia Pereyra, who kindly provided the fungal strains used in this study.

**Conflicts of Interest:** The authors declare no conflict of interest. The funders had no role in the design of the study; in the collection, analyses, or interpretation of the data; in the writing of the manuscript; or in the decision to publish the results.

## References

1. Hermosa, R.; Viterbo, A.; Chet, I.; Monte, E. Plant-beneficial effects of Trichoderma and of its genes. *Microbiology* **2012**, *158*, 17–25. [[CrossRef](#)] [[PubMed](#)]
2. Kubiak-Hardiman, P.; Haughey, S.A.; Meneely, J.; Miller, S.; Banerjee, K.; Elliot, C.T. Identifying gaps and challenges in global pesticide legislation that impact the protection of consumer health: Rice as a case study. *Expo. Health* **2020**, *15*, 597–618. [[CrossRef](#)]
3. La Torre, A.; Iovino, V.; Caradonia, F. Copper in plant protection: Current situation and prospects. *Phytopathol. Mediterr.* **2018**, *57*, 201–236. [[CrossRef](#)]
4. Rai, M.; Bonde, S.; Golinska, P.; Trzcińska-Wencel, J.; Gade, A.; Abd-Elsalam, K.A.; Ingle, A.P. Fusarium as a novel fungus for the synthesis of nanoparticles: Mechanism and applications. *J. Fungi* **2021**, *7*, 139. [[CrossRef](#)] [[PubMed](#)]
5. Abdel-Maksoud, G.; Gaballah, S.; Youssef, A.M.; Eid, A.M.; Sultan, M.H.; Fouda, A. Eco-friendly approach for control of fungal deterioration of archaeological skeleton dated back to the Greco-Roman period. *J. Cult. Herit.* **2023**, *5*, 38–48. [[CrossRef](#)]
6. Sheikh, H.; Awad, M.F. Biogenesis of nanoparticles with inhibitory effects on aflatoxin B1 production by *Aspergillus flavus*. *Electron. J. Biotechnol.* **2022**, *60*, 26–35. [[CrossRef](#)]
7. Kim, D.Y.; Saratale, R.G.; Shinde, S.; Syed, A.; Ameen, F.; Ghodake, G. Green synthesis of silver nanoparticles using laminaria japonica extract: Characterization and seedling growth assessment. *J. Clean. Prod.* **2017**, *172*, 2910–2918. [[CrossRef](#)]
8. Achari, G.; Kowshik, M. Recent developments on nanotechnology in agriculture: Plant mineral nutrition, health, and interactions with soil microflora. *J. Agric. Food Chem.* **2018**, *66*, 8647–8661. [[CrossRef](#)]
9. Guilger, M.; Pasquoto-Stigliani, T.; Bilesky-Jose, N.; Grillo, R.; Abhilash, P.C.; Fraceto, L.F.; de Lima, R. Biogenic silver nanoparticles based on *Trichoderma harzianum*: Synthesis, characterization, toxicity evaluation and biological activity. *Sci. Rep.* **2017**, *7*, 44421. [[CrossRef](#)] [[PubMed](#)]
10. Nandini, B.; Hariprasad, P.; Prakash, H.S.; Shetty, H.S.; Geetha, N. Trichogenic-selenium nanoparticles enhance disease suppressive ability of trichoderma against downy mildew disease caused by *Sclerospora graminicola* in pearl millet. *Sci. Rep.* **2017**, *7*, 2612. [[CrossRef](#)]
11. Lahuta, L.B.; Szablińska-Piernik, J.; Głowacka, K.; Stańkowska, K.; Railean-Plugaru, V.; Horbowicz, M.; Pomastowski, P. The effect of bio-synthesized silver nanoparticles on germination, early seedling development, and metabolome of wheat (*Triticum aestivum* L.). *Molecules* **2022**, *27*, 2303. [[CrossRef](#)]
12. Khan, S.; Singh, S.; Gaikwad, S.; Junnarkar, M.; Pawar, S. Optimization of process parameters for the synthesis of silver nanoparticles from piper betle leaf aqueous extract, and evaluation of their antiphytofungus activity. *Environ. Sci. Pollut. Res.* **2020**, *27*, 27221–27233. [[CrossRef](#)]

13. Fouda, A.; Hassan, S.E.; Abdo, A.M.; El-Gamal, M.S. Antimicrobial, antioxidant and larvicidal activities of spherical silver nanoparticles synthesized by *Endophytic streptomyces* spp. *Biol. Trace Elem. Res.* **2020**, *195*, 707–724. [[CrossRef](#)] [[PubMed](#)]
14. Fouda, A.; Hassan, S.; Eid, A.; Awad, M.; Althumayri, K.; Badr, N.; Hamza, M. Endophytic bacterial strain, *Brevibacillus brevis*-mediated green synthesis of copper oxide nanoparticles, characterization, antifungal, in vitro cytotoxicity, and larvicidal activity. *Green Process Synth* **2022**, *11*, 931–950. [[CrossRef](#)]
15. Rozhin, A.; Batasheva, S.; Kruchkova, M.; Cherednichenko, Y.; Rozhina, E.; Fakhrullin, R. Biogenic silver nanoparticles: Synthesis and application as antibacterial and antifungal agents. *Micromachines* **2021**, *12*, 1480. [[CrossRef](#)] [[PubMed](#)]
16. Guilger-Casagrande, M.; de Lima, R. Synthesis of silver nanoparticles mediated by fungi: A review. *Front. Bioeng. Biotechnol.* **2019**, *7*, 287. [[CrossRef](#)]
17. Balakumaran, M.D.; Ramachandran, R.; Balashanmugam, P.; Mukeshkumar, D.J.; Kalaichelvan, D.T. Mycosynthesis of silver and gold nanoparticles: Optimization, characterization and antimicrobial activity against human pathogens. *Microbiol. Res.* **2018**, *182*, 8–20. [[CrossRef](#)]
18. Syed, A.; Saraswati, S.; Kundu, G.C.; Ahmad, A. Biological synthesis of silver nanoparticles using the *Fungus humicola* sp. and evaluation of their cytotoxicity using normal and cancer cell lines. *Spectrochim. Acta A Mol. Biomol. Spectrosc.* **2013**, *114*, 144–147. [[CrossRef](#)]
19. Zin, N.; Badaluddin, N. Biological functions of *Trichoderma* spp. for agriculture applications. *Ann. Agric. Sci.* **2020**, *65*, 168–178. [[CrossRef](#)]
20. Sanguñedo, P.; Fratila, R.; Estevez, M.B.; Martínez de la Fuente, J.; Grazú, V.; Alborés, S. Extracellular biosynthesis of silver nanoparticles using fungi and their antibacterial activity. *Nano Biomed. Eng.* **2018**, *10*, 165–173. [[CrossRef](#)]
21. Sanguñedo, P.; Estevez, M.B.; Faccio, R.; Alborés, S. Nanopartículas de plata biogénicas a partir del hongo *Punctularia atropurpurascens* para el control de microorganismos. *Mundo Nano* **2019**, *12*, 101–110. [[CrossRef](#)]
22. Cuevas, R.; Durán, N.; Diez, M.; Tortella, G.; Rubilar, O. Extracellular biosynthesis of copper and copper oxide nanoparticles by *stereum hirsutum*, a native white-rot fungus from Chilean forests. *J. Nanomater.* **2015**, *2015*, 1–7. [[CrossRef](#)]
23. Paramelle, D.; Sadovoy, A.; Gorelik, S.; Free, P.; Hobley, J.; Ferning, D.G. A rapid method to estimate the concentration of citrate capped silver nanoparticles from UV-visible light spectra. *Analyst* **2014**, *139*, 4855–4861. [[CrossRef](#)] [[PubMed](#)]
24. CLSI. *Reference Method for Broth Dilution Antifungal Susceptibility Testing of Filamentous Fungi*, 3rd ed.; Approved Standard; CLSI: Wayne, PA, USA, 2017.
25. Melhem, M.S.C.; Coelho, V.C.; Fonseca, C.A.; Oliveira, L.; Bonfietti, L.X.; Szeszs, M.W.; Magri, M.M.C.; Dorneles, F.S.; Taguchi, H.; Moreira, D.V.S.; et al. Evaluation of the sensititre YeastOne and Etest in comparison with CLSI M38-A2 for antifungal susceptibility testing of three azoles, *Amphotericin B*, *Caspofungin*, and *Anidulafungin*, against *Aspergillus fumigatus* and other species, using new clinical breakpoints and epidemiological cutoff values. *Pharmaceutics* **2022**, *14*, 2161. [[CrossRef](#)]
26. Mohammed, S.R.; Zeitar, E.M.; Eskov, I.D. Inhibition of mycelial growth of *Rhizoctonia solani* by chitosan in vitro and in vivo. *Open Agric* **2019**, *13*, 156–161. [[CrossRef](#)]
27. Spagnoletti, F.N.; Spedalieri, C.; Kronberg, F.; Giacometti, R. Extracellular biosynthesis of bactericidal Ag/AgCl nanoparticles for crop protection using the fungus *Macrophomina phaseolina*. *J. Environ. Manag.* **2019**, *231*, 457–466. [[CrossRef](#)] [[PubMed](#)]
28. Di Rienzo, J.; Guzman, A.; Casanove, F.A. Multiple-comparisons method based on the distribution of the root node distance of a binary tree. *JABStatistics* **2002**, *7*, 129–142. [[CrossRef](#)]
29. De Gelder, J.; De Gussem, K.; Vandenebeele, P.; Moens, L. Reference database of Raman spectra of biological molecules. *J. Raman Spectrosc.* **2007**, *38*, 1133–1147. [[CrossRef](#)]
30. Dieing, T.; Ibach, W. Software requirements and data analysis in confocal Raman microscopy. In *Confocal Raman Microscopy*; Dieing, T., Hollricher, O., Toporski, J., Eds.; Springer Series in Optical Sciences; Springer: Berlin/Heidelberg, Germany, 2010; Volume 158. [[CrossRef](#)]
31. Muñoz-Escobar, A.; Reyes-López, S.Y. Antifungal susceptibility of *Candida* species to copper oxide nanoparticles on polycaprolactone fibers (PCL-CuONPs). *PLoS ONE* **2020**, *15*, e0228864. [[CrossRef](#)]
32. Lamichhane, J.R.; Osdaghi, E.; Behlau, F.; Köhl, J.; Jones, J.B.; Aubertot, J.-N. Thirteen decades of antimicrobial copper compounds applied in agriculture. A review. *Agron. Sustain. Dev.* **2018**, *38*, 28. [[CrossRef](#)]
33. Abdussalam-Mohammed, W.; Mohamed, L.; Abrahim, M.S.; Mansour, M.M.A.; Sherif, A.M. Biofabrication of Silver Nanoparticles Using *Teucrium Apollinis* Extract: Characterization, Stability, and Their Antibacterial Activities. *Chemistry* **2023**, *5*, 54–64. [[CrossRef](#)]
34. Fatima, F.; Wahid, I. Eco-friendly synthesis of silver and copper nanoparticles by *Shizophyllum commune* fungus and its biomedical applications. *Int. J. Mol. Sci. Technol.* **2021**, *19*, 7915–7926. [[CrossRef](#)]
35. Ovais, M.; Khalil, A.T.; Ayaz, M.; Ahmad, I.; Nethi, S.K.; Mukherjee, S. Biosynthesis of metal nanoparticles via microbial enzymes: A mechanistic approach. *Int. J. Mol. Sci. Technol.* **2018**, *19*, 4100. [[CrossRef](#)] [[PubMed](#)]
36. Mishra, S.; Singh, B.; Singh, A.; Keswani, C.; Naqvi, A.; Singh, H. Biofabricated silver nanoparticles act as a strong fungicide against *bipolaris sorokiniana* causing spot blotch disease in wheat. *PLoS ONE* **2018**, *9*, e97881. [[CrossRef](#)] [[PubMed](#)]
37. Panpatte, D.; Jhala, Y. Advances for sustainable agriculture. In *Nanotechnology for Agriculture*; Springer: Berlin/Heidelberg, Germany, 2019. [[CrossRef](#)]
38. Ramírez-Valdespino, C.A.; Orrantia-Borunda, E. *Trichoderma* and nanotechnology in sustainable agriculture: A review. *Front. Fungal Biol.* **2021**, *2*, 764675. [[CrossRef](#)]

39. Fayaz, A.M.; Balaji, K.; Girilal, M.; Yadav, R.; Kalaichelvan, P.T.; Venketesan, R. Biogenic synthesis of silver nanoparticles and their synergistic effect with antibiotics: A study against gram-positive and gram-negative bacteria. *Nanomed. Nanotechnol. Biol. Med.* **2010**, *6*, 103–109. [[CrossRef](#)]
40. Estevez, M.B.; Mitchell, S.G.; Faccio, R.; Alborés, S. Biogenic silver nanoparticles: Understanding the antimicrobial mechanism using Confocal Raman Microscopy. *Mater. Res. Express* **2020**, *6*, 1250f5. [[CrossRef](#)]
41. Awwad, A.; Amer, M. Biosynthesis of copper oxide nanoparticles using *Ailanthus altissima* leaf extract and antibacterial activity. *Chem. Int.* **2020**, *6*, 210–217. [[CrossRef](#)]
42. Wilson, B.K.; Prud'homme, R.K. Nanoparticle size distribution quantification from transmission electron microscopy (TEM) of ruthenium tetroxide stained polymeric nanoparticles. *J. Colloid. Interface Sci.* **2021**, *604*, 208–220. [[CrossRef](#)] [[PubMed](#)]
43. Souza, T.; Ciminelli, V.; Mohallem, N. A comparison of TEM and DLS methods to characterize size distribution of ceramic nanoparticles. *J. Phys.* **2016**, *733*, 012039. [[CrossRef](#)]
44. Estevez, M.B.; Casaux, M.L.; Fraga, M.; Faccio, R.; Alborés, S. Biogenic Silver Nanoparticles as a Strategy in the Fight Against Multi-Resistant *Salmonella enterica* Isolated From Dairy Calves. *Front. Bioeng. Biotechnol.* **2021**, *9*, 644014. [[CrossRef](#)]
45. Joseph, E.; Singhvi, G. Chapter 4—Multifunctional nanocrystals for cancer therapy: A potential nanocarrier. In *Nanomaterials for Drug Delivery and Therapy*; Grumezescu, A.M., Ed.; William Andrew Publishing: Norwich, NY, USA, 2019; pp. 91–116. [[CrossRef](#)]
46. Estevez, M.B.; Raffaelli, S.; Mitchell, S.G.; Faccio, R.; Alborés, S. Biofilm eradication using biogenic silver nanoparticles. *Molecules* **2020**, *25*, 2023. [[CrossRef](#)]
47. Guilger-Casagrande, M.; Germano-Costa, T.; Bilesky-José, N.; Pasquoto-Stigliani, T.; Carvalho, L.; Fraceto, L.F.; de Lima, R. Influence of the capping of biogenic silver nanoparticles on their toxicity and mechanism of action towards *Sclerotinia sclerotiorum*. *J. Nanobiotechnol.* **2021**, *19*, 53. [[CrossRef](#)] [[PubMed](#)]
48. Ahluwalia, V.; Kumar, J.; Sisodia, R.; Shakil, N.; Walia, S. Green synthesis of silver nanoparticles by *Trichoderma harzianum* and their bio-efficacy evaluation against *Staphylococcus aureus* and *Klebsiella pneumoniae*. *Ind. Crops Prod.* **2014**, *55*, 202–206. [[CrossRef](#)]
49. Noshad, A.; Iqbal, M.; Folkers, L.; Hetherington, C.; Khan, A.; Numan, M.; Ullah, S. Antibacterial Effect of Silver Nanoparticles (AgNPs) Synthesized from *Trichoderma Harzianum* against *Clavibacter Michiganensis*. *Nano Res.* **2019**, *58*, 10–19. [[CrossRef](#)]
50. Konappa, N.; Udayashankar, A.; Dhamodaran, N.; Krishnamurthy, S.; Jagannath, S.; Uzma, F.; Pradeep, C.K.; De Britto, S.; Chowdappa, S.; Jogaiah, S. Ameliorated Antibacterial and Antioxidant Properties by *Trichoderma harzianum* Mediated Green Synthesis of Silver Nanoparticles. *Biomolecules* **2021**, *11*, 535. [[CrossRef](#)] [[PubMed](#)]
51. Sundaravadivelan, C.; Padmanabhan, M. Effect of mycosynthesized silver nanoparticles from filtrate of *Trichoderma harzianum* against larvae and pupa of dengue vector *Aedes aegypti* L. *Environ. Sci. Pollut. Res.* **2014**, *21*, 4624–4633. [[CrossRef](#)] [[PubMed](#)]
52. Shende, S.; Ingle, A.P.; Gade, A.; Raid, M. Green synthesis of copper nanoparticles by *Citrus medica* Linn. (Idilimbu) juice and its antimicrobial activity. *World J. Microbiol. Biotechnol.* **2015**, *31*, 865–873. [[CrossRef](#)] [[PubMed](#)]
53. Ahmad, H.; Venugopal, K.; Bhat, A.H.; Kavitha, K.; Ramanan, A.; Rajagopal, K.; Srinivasan, R.; Manikandan, E. Enhanced Biosynthesis Synthesis of Copper Oxide Nanoparticles (CuO-NPs) for their Antifungal Activity Toxicity against Major Phyto-Pathogens of Apple Orchards. *Pharm. Res.* **2020**, *37*, 246. [[CrossRef](#)]
54. Zia, R.; Riaz, M.; Farooq, N.; Qamar, A.; Anjum, S. Antibacterial activity of Ag and Cu nanoparticles synthesized by chemical reduction method: A comparative analysis. *Mater. Res. Express* **2018**, *5*, 075012. [[CrossRef](#)]
55. Usman, M.; Farooq, M.; Wakeel, A.; Nawaz, A.; Cheema, S.A.; ur Rehman, H.; Ashraf, I.; Sanaullah, M. Nanotechnology in agriculture: Current status, challenges and future opportunities. *Sci. Total Environ.* **2020**, *721*, 137778. [[CrossRef](#)] [[PubMed](#)]
56. Oluwaseun, A.; Sarin, N.B. Impacts of biogenic nanoparticle on the biological control of plant pathogens. *Adv. Biotechnol. Micro* **2017**, *7*, 555711. [[CrossRef](#)]
57. Martínez, S. Stem rot management by nitrogen and potassium fertilization and effect on grain yield and quality of rice in Uruguay. *Can. J. Plant Pathol.* **2021**, *41*, 783–793. [[CrossRef](#)]
58. Rangarani, A.; Rajan, C.P.D.; Sarada Jayalakshmi Devi, R.; Lakshmi Narayana Reddy, V.; Sudhakar, P. Evaluation of fungicides on *Sclerotium oryzae*, incitant of rice stem rot disease. *J. Pharmacogn. Phytochem.* **2018**, *7*, 01–03.

**Disclaimer/Publisher's Note:** The statements, opinions and data contained in all publications are solely those of the individual author(s) and contributor(s) and not of MDPI and/or the editor(s). MDPI and/or the editor(s) disclaim responsibility for any injury to people or property resulting from any ideas, methods, instructions or products referred to in the content.